

Multi-parameter analysis of air flow velocity on peach precooling efficiency using CFD

Chen, Y. M., *Song, H. Y. and Su, Q.

College of Agricultural Engineering, Shanxi Agricultural University,
 Taigu 030800, Shanxi Province, China

Article history

Received:

14 April 2020

Received in revised form:

21 March 2021

Accepted:

14 October 2021

Keywords

airflow rate,
 internal heat source,
 forced-air cooling (FAC),
 computational fluid
 dynamics (CFD),
 mass loss

Abstract

In the present work, a three-dimensional computational fluid dynamics (CFD) model was established to simulate the heat transfer process at different air-inflow velocities, and to predict the spatial and temporal variations of temperature distribution during forced-air cooling (FAC). Based on the conventional evaluation system, a more comprehensive multi-parameter evaluation system was proposed to determine an optimal precooling strategy of various air-inflow velocities. The current system employed a novel heterogeneity index to quantify the overall uniformity (OHI), and added a detailed theoretical calculation procedure of the cumulative moisture loss during the forced-convection cooling (M, mg). By analysing the effect of different airflow rates on SECT, precooling uniformity, moisture loss, and energy requirement, an airflow rate in the range of 1.5 - 2.5 m·s⁻¹ was recommended as optimum for harvested peach precooling. Any further increase in air-inflow velocity led to excessive energy cost since it generated a relatively low decrease in SECT and overall heterogeneity index, so as moisture loss. At the same time, the moisture loss of peach primarily occurred in HCT, which was inversely proportional to airflow rate and cooling uniformity. An increasing power-law function relationship existed between energy consumption and airflow rate. The present work demonstrated the effect of various air-inflow velocities on peach precooling efficiency, and provided an integral evaluation system to optimise the precooling strategy of other horticultural fruits.

© All Rights Reserved

Introduction

Peach is a kind of spherical fruit with thin skin, soft flesh, and high water content. Peach is abundant in the Yangtze River Delta of China and the southern regions of Shanxi and Shandong provinces. Peach-picking season is in the hot and rainy period of June to August. During this period, the large amount of field heat contained in freshly harvested peach keeps it with high respiration intensity and ethylene release, which fundamentally accelerates the metabolism and after-ripening speed, thus giving peach poor storage resistance and high perishability (Lurie and Crisosto, 2005). However, precooling, the process of promptly eliminating the field heat from fresh fruits prior to the postharvest cold chain, is a critical technique in inhibiting enzymatic activity and microbial growth, and also ensuring the quality and safety (Ravindra and Goswami, 2008). Therefore, to maximise commercial peach marketability, postharvest peach must be rapidly and effectively pre-cooled, and then

maintained in refrigerated storage (Becker *et al.*, 1996).

To efficiently cool horticultural products, forced-air cooling (FAC) is commonly used (Dehghannya *et al.*, 2010). The main principle refers to the rotate speed of the axial fan at different frequencies which will cause the air in a cooling channel to go through the vents on both sides of the container at different flow rates, consequently forming different pressures at the vents on both sides, thus the refrigerated airflow and fruit surface can directly conduct the process of heat and mass transfer (Tutar *et al.*, 2009). Therefore, different airflow rates form different magnitudes of convective heat transfer coefficient. During the precooling process of fruits, the velocity of air flowing to the windward side of the carton is the air-inflow velocity. Meanwhile, the velocity of air flowing through the fruits inside the carton and flowing out along the vents on the back of the carton is the air-outflow velocity, as shown in Figure 1. Defraeye *et al.* (2013) reported that the

*Corresponding author.
 Email: yybbao2003@163.com

optimisation of cooling strategy mainly involves in determining an appropriate range of air-inflow velocity, which is required to increase the throughput by narrowing the cooling time, aiming to decrease postharvest losses and prolong shelf life, and to limit operational costs and energy consumption in precooling system. However, most research mainly investigated the characteristics of heat and mass

transfer or sensory quality of peach in the process of refrigeration or freezing, whereas only few research was done on peach precooling efficiency, thus generating an unclear effect on peach precooling efficiency of different cooling strategies (Becker *et al.*, 1996; Shinya *et al.*, 2014; Yu *et al.*, 2016; Zhou *et al.*, 2019).

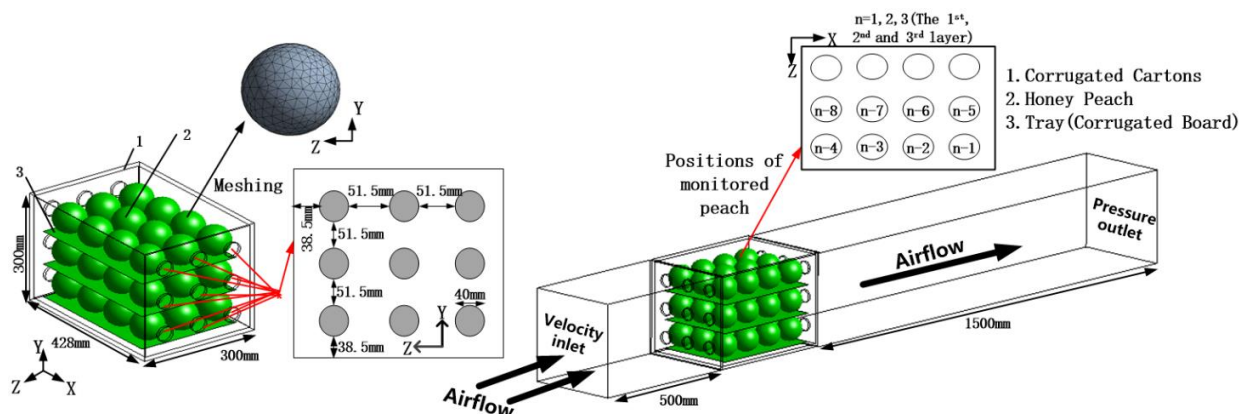


Figure 1. Schematic diagram for fruit package design and boundary conditions for a single carton: positions of monitored peach inside individual packaging (from n-1 to n-8, where n = 1, 2, and 3).

Computational fluid dynamics (CFD) has been widely applied in all aspects of cold chain processing, as airflow pattern and temperature can be obtained at high spatial and temporal resolutions. The method of CFD numerical simulation was successfully used in previous research for optimising the design of precooling packaging crates for various fruits and vegetables. In addition, different evaluation systems were also provided, containing the cooling time, energy demand, precooling uniformity, airflow resistance, and mechanical strength (Delele *et al.*, 2013b; Berry *et al.*, 2016; O'Sullivan *et al.*, 2017; Wu *et al.*, 2018). Additionally, the accuracy of CFD simulation was successfully confirmed with great agreement in experimental data, as reflected in the lower standard error and root-mean-square error ($< 1^{\circ}\text{C}$) (Dehghannya *et al.*, 2011; Defraeye *et al.*, 2013; Delele *et al.*, 2013a; O'Sullivan *et al.*, 2016; Han *et al.*, 2017b).

Unfortunately, these numerical models were simulated without the consideration of internal heat source. This affects the evaluation of various fresh fruits and vegetables cooling efficiency (Dehghannya *et al.*, 2008; Zhao *et al.*, 2016), especially for perishable fruits (Becker *et al.*, 1996) such as peach or strawberry. Furthermore, the above-mentioned studies seldom made detailed theoretical calculation on the specific amount of moisture loss, and rarely

analysed the effect of various airflow rates (*i.e.*, $0 - 3 \text{ m}\cdot\text{s}^{-1}$) on mass loss. Besides, in conventional evaluation system, the temperature heterogeneity index (HI) is popularly used to compare the uniformity at single time point, which is challenging to employ at a specific value to quantify the overall uniformity in the total precooling process, and also hard to achieve instantaneous visual expression of the fruit chilling injury or moisture loss (Olatunji *et al.*, 2017).

To overcome these shortcomings and further improve the simulation accuracy, the present work created a reliable CFD model to simulate the three-dimensional temporal and spatial distributions of airflow and temperature considering the internal heat source. At the same time, a more integral multi-parameter evaluation system (*i.e.*, dimensionless temperature, precooling uniformity, energy consumption, and cumulative moisture loss) was proposed to determine an optimal air-inflow velocity range for peach precooling, and to understand the functional relationship between peach cooling performance and air-inflow velocity. The present work aimed to extremely improve the peach edible value without incurring excessive energy demand, and to provide a reliable theoretical reference for optimising the cooling strategy of other horticultural fruits.

Materials and methods

Physical model and meshing

The physical model of FAC was established by ANSYS Design Modeler 19.2 (Figure 1). The vent design of this model was proposed based on recent similar design which was successfully applied in the fruit postharvest cold chain (Delele *et al.*, 2013b). Meanwhile, the total ventilated area percentage (TVA) of this corrugated carton is fundamentally consistent with the recommendations from Berry *et al.* (2015) who found that most of corrugated cartons used for export have an average TVA of 4%. Individual corrugated carton, containing three identically trays ($368 \times 256 \times 4 \text{ mm}^3$), was created with the geometrical dimension of $428 \times 300 \times 300 \text{ mm}^3$ and thickness of 7 mm. Moreover, during the process of numerical simulation, Defraeye *et al.* (2013) recommended that the length of upstream and downstream sections should be large enough in order to avoid the effect of boundary conditions, at inlet and outlet, on the airflow in the proximity of the carton.

To limit the computational cost, some simplifications were required to be performed to the simulation model. Each carton held 36 peaches packed across three layers of trays, and peaches were modelled discretely as spheres with a diameter of 80 mm. The complex geometry was divided into unstructured meshes with the application of the Meshing software. The total number of meshes was 6.9×10^6 with a maximum edge length of 1 mm. Through the mesh quality inspection, the skewness of the whole model was found to be lower than 0.9 (*i.e.*, with high and rational mesh quality).

Mathematical model

The three-dimensional computational domain of this fluid dynamic model was primarily made of two distinct sub-domains (*i.e.*, the zone of free-airflow and fruit). Regarding free-airflow zone, the airflow was obtained by solving the Reynolds-averaged Navier-Stokes equations (Eqs. 1, 2, 3) (Ferrua and Singh, 2009):

Mass conservation equation:

$$\text{div}(U) = 0 \quad (\text{Eq. 1})$$

Momentum conservation equation:

$$\frac{\partial(\rho_a u)}{\partial t} + \text{div}(\rho_a u U) = \text{div}(\mu_a \text{grad} u) - \frac{\partial P}{\partial x} + S_u \quad (\text{Eq. 2a})$$

$$\frac{\partial(\rho_a v)}{\partial t} + \text{div}(\rho_a v U) = \text{div}(\mu_a \text{grad} v) - \frac{\partial P}{\partial y} + S_v \quad (\text{Eq. 2b})$$

$$\frac{\partial(\rho_a w)}{\partial t} + \text{div}(\rho_a w U) = \text{div}(\mu_a \text{grad} w) - \frac{\partial P}{\partial z} + S_w \quad (\text{Eq. 2c})$$

Energy conservation equation:

$$\frac{\partial T_a}{\partial t} + \text{div}(U T_a) = \text{div}\left(\frac{\lambda_a}{\rho_a c_a} \text{grad} T_a\right) \quad (\text{Eq. 3})$$

where, U = velocity vector; u, v, w = velocity component in the x, y, z direction, respectively ($\text{m}\cdot\text{s}^{-1}$); ρ_a and λ_a = density ($\text{kg}\cdot\text{m}^{-3}$) and thermal conductivity ($\text{W}\cdot\text{m}^{-1}\cdot\text{K}^{-1}$) of air, respectively; μ_a = dynamic viscosity ($\text{Pa}\cdot\text{s}$); c_a = air-specific heat capacity ($\text{J}\cdot\text{kg}^{-1}\cdot\text{K}^{-1}$); P = water vapour pressure inside the carton (Pa); T_a = fluid temperature (K); S_u, S_v, S_w = generalised source terms in the $x, y,$ and z direction, respectively; $S_u = S_w = 0, S_v = -\rho_a g$; and g = acceleration due to gravity ($9.81 \text{ m}\cdot\text{s}^{-2}$).

For fruit zone, the internal heat source ($Q_{\text{int}}, \text{W}\cdot\text{m}^{-3}$) was mainly made up of respiration (Q_r, W) and transpiration heat (Q_t, W), which were loaded into the heat conduction differential governing equation of fruit zone (Eqs. 4 and 5):

$$\lambda_p \left(\frac{\partial^2 T_{p,t}}{\partial r^2} + \frac{2}{r} \frac{\partial T_{p,t}}{\partial r} + \frac{\cos \theta}{r^2 \sin \theta} \cdot \frac{\partial T_{p,t}}{\partial \theta} + \frac{1}{r^2} \frac{\partial^2 T_{p,t}}{\partial \theta^2} \right) + Q_{\text{int}} = c_p \rho_p \frac{\partial T_{p,t}}{\partial t} \quad (\text{Eq. 4})$$

$$Q_{\text{int}} = (Q_r - Q_t) / V_p \quad (\text{Eq. 5})$$

where, $T_{p,t}$ = fruit temperature at time t (K), ρ_p and λ_p = fruit density ($\text{kg}\cdot\text{m}^{-3}$) and thermal conductivity ($\text{W}\cdot\text{m}^{-1}\cdot\text{K}^{-1}$), respectively, c_p = specific heat capacity of fruit ($\text{J}\cdot\text{kg}^{-1}\cdot\text{K}^{-1}$), A_p and V_p = fruit surface area (m^2) and volume (m^3), respectively, and r = vector radius of spherical fruit (m).

A detail calculation of the heat of respiration and transpiration was obtained using Eqs. 6 and 7:

$$Q_r / V_p = \rho_p \times f_p \quad (\text{Eq. 6})$$

$$Q_t / V_p = L_p m_p A_p / V_p = 3 L_p m_p / r \quad (\text{Eq. 7})$$

where, f_p = respiratory heat generation per unit mass of produce ($\text{W}\cdot\text{kg}^{-1}$), namely $f_p = (10.7/3600) \times A \times [1.8(T_{p,t} - 273.15) + 32]^B$. Among them, the coefficients of respiration (*i.e.*, A and B) for various commodities were tabulated by Becker *et al.*

(1996), and successfully applied in previous research (Rennie and Tavoularis, 2009; Han *et al.*, 2017a). Thus, the peach respiration coefficients was defined as 1.2996×10^{-5} and 3.6417 , respectively. $L_p = 9.1T_{p,t}^2 - 7512.9T_{p,t} + 3875100$ = latent evaporation heat ($J \cdot kg^{-1}$), and m_p = transpiration rate per unit area of fruit surface ($kg \cdot m^{-2} \cdot s^{-1}$), which was induced by a difference in water vapour pressure between fruit surface and surrounding air.

$$m_p = k_p(P_p - P_a) \quad (\text{Eq. 8})$$

where, the water vapour pressure at fruit evaporation surface (P_p , Pa) was obtained by $P_p = VPL \cdot P_W(T_{awa})$, and among them, $P_W(T_{awa})$ was the water vapour saturation pressure estimated at fruit surface average temperature (Eqs. 9 and 20), and vapour pressure lowering (VPL) effect of various commodities were also provided by Becker *et al.* (1996) for peach, $VPL = 0.99$. The partial water vapour pressure (P_a , Pa) in the refrigerated air is defined as $P_a = RH \cdot P_W(T_a)$ (Dehghannya *et al.*, 2008). In addition, the relative humidity (RH) of airflow was set to 90% in the proposed model.

$$P_W = \exp\left(23.4795 - \frac{3990.5}{T - 39.317}\right) \quad (\text{Eq. 9})$$

Meanwhile, the mass transfer coefficient (k_p , $kg \cdot m^{-2} \cdot s^{-1} \cdot Pa^{-1}$) was obtained using Eq. 10:

$$k_p = \frac{1}{1/k_a + 1/k_s} \quad (\text{Eq. 10})$$

where, k_s = skin mass transfer coefficient for peach (Becker *et al.*, 1996), and $k_s = 14.2 \times 10^{-9}$ ($kg \cdot m^{-2} \cdot s^{-1} \cdot Pa^{-1}$). The value of air film mass transfer coefficient (k_a) was calculated by employing the Sherwood-Reynolds- Schmidt correlations (Zhao *et al.*, 2016):

$$Sh = \frac{k_a \cdot 2r \cdot R_{H_2O} \cdot T_a}{\delta M_{H_2O}} = 2.0 + 0.552Re^{0.53}Sc^{0.33} \quad (\text{Eq. 11})$$

$$\delta = \frac{9.1 \times 10^{-9} \times T_a^{2.5}}{T_a + 245.18} \quad (\text{Eq. 12})$$

where, Sh , Re , and Sc = number of Sherwood, Reynolds, and Schmidt, respectively; M_{H_2O} = molecular mass of water vapour ($0.018 kg \cdot mol^{-1}$); and R_{H_2O} = water vapour constant ($8.314 J \cdot mol^{-1} \cdot K^{-1}$). Assuming negligible low airflow surrounded the fruit, namely, $Re \approx 0$ (Rennie and Tavoularis, 2009); at this point, k_a was estimated using Eq. 13:

$$k_a = \delta M_{H_2O} / (R_{H_2O} T_a r) \quad (\text{Eq. 13})$$

Consequently, when $T_a = 275.15$ K, the diffusion coefficient of water vapour in air was $\delta = 2.196 \times 10^{-5} m^2 \cdot s^{-1}$. Furthermore, k_a and k_p was 4.320×10^{-9} and 3.313×10^{-9} ($kg \cdot m^{-2} \cdot s^{-1} \cdot Pa^{-1}$), respectively.

Numerical setup

Initial temperature within fruit computational domain was set to 299.15 K, and the air-inflow temperature was taken as the refrigerated air temperature of 275.15 K. Representatively, the inlet boundary condition was defined as a velocity inlet, and air outlet of the computational domain was defined as a pressure-outflow boundary (Figure 1). In addition, no-slip velocity boundary conditions were set at fruit and carton wall surfaces.

The standard k- ϵ turbulence model was performed to run the transient simulation (Norton *et al.*, 2007). The heat of respiration and transpiration was loaded into the fruit zone by a user-define function (UDF) written in the C programming language. Second-order upwind scheme was employed to explain the influence of natural convection terms, and the algorithm of semi-implicit method for pressure-linked equations (SIMPLE) was involved for pressure-velocity coupling (Berry *et al.*, 2016). A convergence criterion of 10^{-4} was set for continuity, momentum, and turbulence, whereas 10^{-6} was set for performing energy equation. Table 1 defines the thermophysical properties of air and solid materials. The simulation was implemented in a 64-bit windows 10 computer with a 2.90 GHZ Intel® Core i7-7500 CPU and 8GB RAM.

Table 1. Parameters of thermal-physical properties.

Parameter	Density ($kg \cdot m^{-3}$)	Specific heat capacity ($J \cdot kg^{-1} \cdot K^{-1}$)	Thermal conductivity ($W \cdot m^{-1} \cdot K^{-1}$)	Dynamic viscosity ($Pa \cdot s$)
Precooling-air	1.293	1,006	0.02343	1.73e-5
Peach	691.95	3,898.3	0.472	-
Corrugated carton	220	1,700	0.065	-
Tray (corrugated board)	260	1,700	0.065	-

Multi-parameter evaluation system

Dimensionless temperature

In general, the change of normalised dimensionless temperature (Y) with cooling time was expressed using Eq. 14, which was used to obtain specific cooling time, namely, the HCT and SECT in min, defined as half ($Y = 1/2$) and seven-eighths ($Y = 1/8$) cooling time, respectively (Dincer, 1995). Fruit cooling rate was evaluated by comparing the value of SECT, which was the time required for cooling the product to seven-eighths temperature.

$$Y = \frac{T_p - T_a}{T_{pin} - T_a} \quad (\text{Eq. 14})$$

where, T_p = fruit temperature at a certain time (t); T_{pin} = initial fruit temperature (299.15 K); and T_a = precooling-air temperature set for the FAC room (275.15 K).

Cooling uniformity

A variation curve of ΔY is a novel representation of cooling uniformity as a function of the dimensionless cooling time (Y_{avg}). When compared with the temperature variability which has been reported as the relative standard deviation (Defraeye *et al.*, 2015a), the new heterogeneity index not only can observe the instantaneous uniformity (HI'_t) at single time point, but also intuitively judge the overall heterogeneity index (*i.e.*, $OHI = \Delta Y_{max} - \Delta Y_{min}$) by using a specific value. A lower value of OHI represents a high level of temperature homogeneity (Olatunji *et al.*, 2017).

$$Y_{avg,t} = \sum_{n=1}^m Y_{n,t} / m \quad (\text{Eq. 15})$$

$$\Delta Y_{n,t} = Y_{n,t} - Y_{avg,t} \quad (\text{Eq. 16})$$

$$HI'_t = \Delta Y_{max-P,t} - \Delta Y_{min-N,t} \quad (\text{Eq. 17})$$

$$HI_t = \frac{1}{T_{avg,t}} \sqrt{\frac{1}{m-1} \sum_{n=1}^m (T_{n,t} - T_{avg,t})^2} \quad (\text{Eq. 18})$$

where, $T_{n,t}$ = temperature of peach n ; $T_{avg,t}$ = average temperature, $Y_{avg,t}$ = average over all $Y_{n,t}$ at time t . At this point, $\Delta Y_{max-P,t}$ or $\Delta Y_{min-N,t}$ = maximum positive or minimum negative number of $\Delta Y_{n,t}$ which reflected that the horticultural commodity was higher or lower than the average temperature, consequently cooling slowly (hot spots) or quickly (cold spots).

Energy consumption

The relationship between energy consumption (E_w) and cooling time remains a key factor in evaluating the cooling efficiency during the commercial FAC (Thompson *et al.*, 2010). Total energy consumption was calculated using Eq. 19 when cooling a single carton packed with products (Defraeye *et al.*, 2015b).

$$E_w = P_w \cdot t \quad (\text{Eq. 19})$$

where, P_w (W) = power of the fan, which can be estimated from the pressure drop (ΔP , Pa) and volume flow rate (G , $m^3 \cdot s^{-1}$). The functional relationship was $P_w = \Delta P \cdot G$ (O'Sullivan *et al.*, 2017).

Fruit mass loss

Integrated evaluation of precooling efficiency is essential for optimising the cooling strategy of horticultural products, and ensuring optimum fresh quality and safety (Kongwong *et al.*, 2019). Therefore, to realise a comprehensive analysis of precooling efficiency, an influence of various air-inflow velocities on mass degradation (*i.e.*, the accumulated moisture loss in HCT and SECT) had to be considered. Peach mass loss (M , mg) mainly occurred by transportation driving force, which was estimated by Eq. 21 (Hoang *et al.*, 2003); $M = \sum(m_p \times A_p)$. Among them, the rate of moisture loss (m_p , $kg \cdot m^{-2} \cdot s^{-1}$) was calculated using Eqs. 8 to 13.

$$T_{awa} = \frac{1}{A_p} \sum_{i=1}^N A_i T_i \quad (\text{Eq. 20})$$

$$-\frac{\partial M}{\partial t} = m_p \times A_p \quad (\text{Eq. 21})$$

where, A_i = area of mesh cell i ; A_p = fruit surface area (m^2); T_i = fruit temperature at cell position $I = 1$ to $I = N$; and T_{awa} = surface area-weighted average temperature (K).

Results and discussion

To deeply analyse the feasibility of this evaluation system for optimising peach cooling strategy in the present work, the dynamics simulation was adopted with the CFD code ANSYS Fluent 19.2 for six various air-inflow velocities (*i.e.*, 0.5, 1, 1.5, 2, 2.5, and $3 m \cdot s^{-1}$).

Dimensionless temperature

Figure 2a shows the cooling rate with respect to the dimensionless temperature *versus* cooling time. The increasing airflow rate caused the slope of dimensionless temperature curve to become steeper, which was reflected in the fastest increase in cooling rate occurring at the airflow rate between 0.5 and 1 m·s⁻¹ (Δ HCT = 15.52 min, Δ SECT = 37.60 min). However, although the SECT was shortened by 15.71 min when the airflow rate was increased from 2 to 2.5 m·s⁻¹, there were only small differences between 1, 1.5, and 2 m·s⁻¹, namely < 2.97% for HCT and < 5.52% for SECT, whereas when $V_{inlet} > 2.5$ m·s⁻¹, neither the HCT nor SECT significantly decreased.

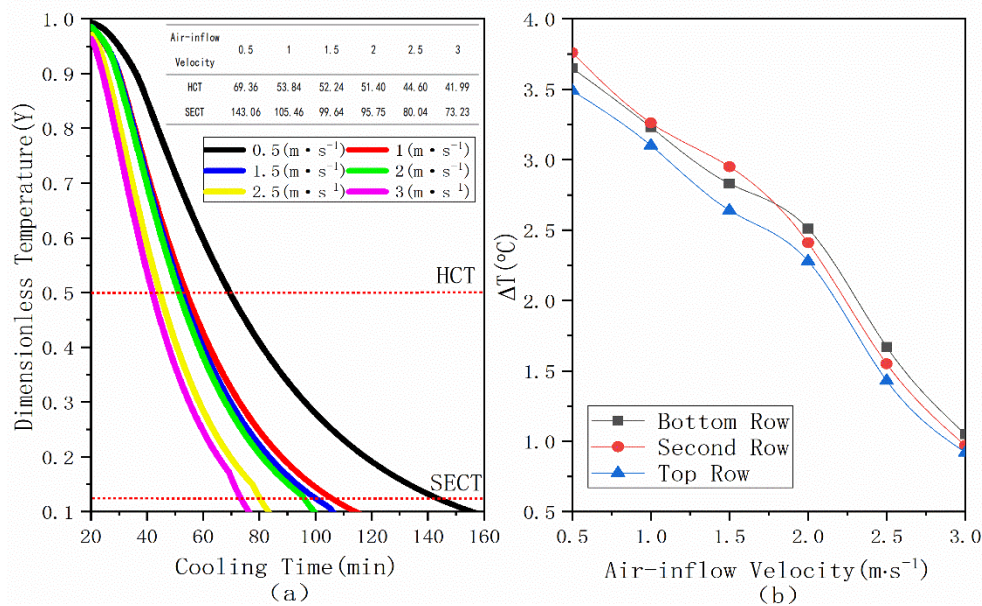


Figure 2. (a) Dimensionless temperature as a function of cooling time for different air-inflow velocities: monitoring position is the core temperature of peach (1-2); and (b) temperature discrepancy of peach located at the inlet and outlet of each layer when the simulation time of 80 min: $\Delta T = T_{n-1} - T_{n-4}$, where $n = 1, 2$, and 3 .

Cooling uniformity

As shown in Figure 3, the two bell ($|\Delta Y|$) curves yielded heterogeneity plot with a characteristic ‘eye’ shape. Hot ($\Delta Y_{max-P,t}$) and cold ($\Delta Y_{min-N,t}$) spots in that shape were normally distributed, with a lower level of heterogeneity, which is in line with the description of superior heterogeneity for system B proposed by Olatunji *et al.* (2017). Hence, for the different air-inflow velocities, this novel process progression index can be used commendably to quantify and visualise the cooling uniformity of peach over the entire precooling process.

The difference of the overall uniformity (OHI) between 0.5 and 1.5 m·s⁻¹ was 0.011, namely only 6.11% for its improvement rate, thus indicating no

This clearly indicated that there was little significant reduction in HCT and SECT when $V_{inlet} > 1$ m·s⁻¹. Besides, O’Sullivan *et al.* (2016) performed experimental verification of such similar decrease in cooling rate for kiwifruit. In addition, the HCT and SECT for peach located at the back was longer as compared to that for peach at the front of the pallet layer. However, discrepancy of HCT and SECT for peaches located at the front and back of the pallet layer was becoming smaller with an increase in air-inflow velocity (Figure 2b). The reason was that the difference in cooling time between peaches was caused by temperature discrepancy.

remarkable influence on uniformity when the airflow rate was increased from 0.5 to 1.5 m·s⁻¹. However, when the airflow rate was increased from 1.5 to 2.5 m·s⁻¹, the decrease amplitude of its heterogeneity index (Δ OHI = 0.032) was approximately three-fold of that in 0.5 - 1.5 m·s⁻¹, thus indicating that the overall cooling uniformity of 0.5 - 1.5 m·s⁻¹ was slightly worse than that of other airflow rates. Therefore, it could be more suitable to maintain the peach quality when $V_{inlet} > 1.5$ m·s⁻¹, as uniform cooling of horticultural products promotes uniformity quality (Nahor *et al.*, 2005; O’Sullivan *et al.*, 2017). Additionally, this exhibits a similar trend that an increase in airflow rate can increase cooling uniformity (de Castro *et al.*, 2004).

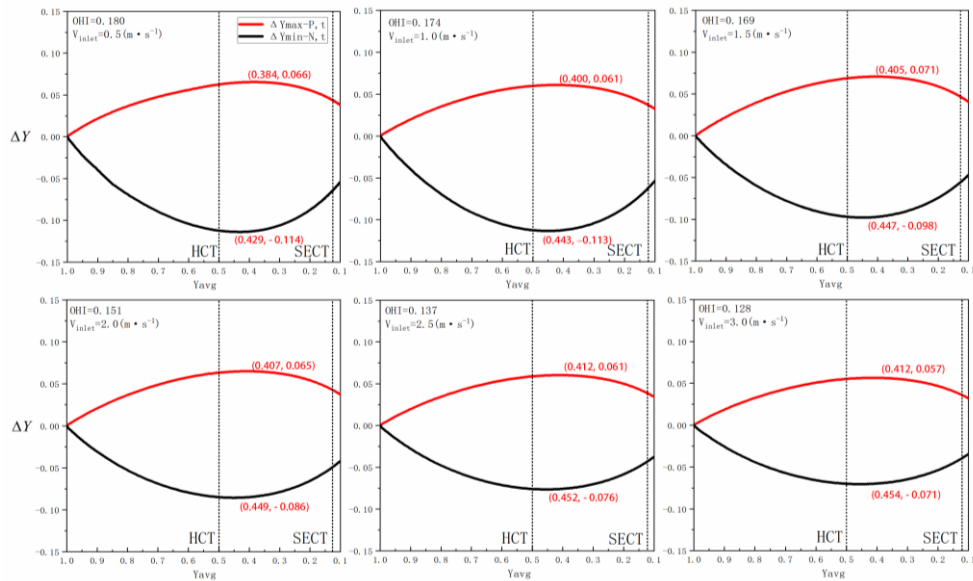


Figure 3. The ΔY of individual carton as a function of Y_{avg} for different air-inflow velocities.

The obtained result could be mainly attributed to the fact that a successive increase in air-inflow velocity makes the airflow more quickly and evenly distributed across the container, thus generating less airflow resistance and more efficient heat exchange between peach and refrigerated air. Another reason was lower airflow rate could have led to a higher temperature discrepancy between the peaches at inlet and outlet of each layer (Figure 2b). This thus led to a secondary pollution induced by mutual heat transfer between peaches.

Energy consumption and moisture loss of fruit

When the cooling time is equal to the SECT, fruits can be transferred to storage equipment or cold chain logistics, where the remaining field heat can be removed with less energy consumption (Brosnan and Sun, 2001). Therefore, during this period, the total energy consumed by the fan (E_w , $\times 10^6$ J) should be calculated for fairly comparing the cooling efficiency on different airflow rates. The progressive increase of airflow rate exerted a significant impact on the growth of E_w as seen in Figure 4a, thus indicating consistency with the non-linear growth trend described by Berry *et al.* (2016). Moreover, the E_w in SECT was nearly two-fold of that in HCT, and the E_w in SECT *versus* the airflow rate can be fitted as a power-law function ($E_w = aV^b$). Among them, $a = 1.434$ and $b = 2.533$, and its adjusted correlation coefficient (R^2) was 0.9993. This is basically similar to the changing trend of E_w ($a = 1.7666$, $b = 2.3680$) fitted for the palletised apples by Han *et al.* (2018), as

the root-mean-square error (RMSE) between the two fitting functions was 0.622. Furthermore, above 2.5 $m \cdot s^{-1}$, the relative decrease in cooling time ($\Delta HCT < 2.61$ min and $\Delta SECT < 6.81$ min) and uniformity ($\Delta OHI < 6.57\%$) remained relatively minor in comparison with the drastic increase in energy consumption (Figures 2a, 3, and 4a). This result coincides with observations by Han *et al.* (2017b), thus recommending that the air-inflow velocities for individual apple cooling should not exceed 2.5 $m \cdot s^{-1}$. Therefore, to ensure prompt and uniform precooling without inducing excessive energy waste, the better range of airflow rate was suggested to be at 1.5 - 2.5 $m \cdot s^{-1}$.

In addition, during SECT, the relative reduction in water evaporation of single peach between 0.5 and 1.5 $m \cdot s^{-1}$ ($\Delta M_{SECT} = 106.04$) was nearly three-fold of that in 1.5 - 2.5 $m \cdot s^{-1}$ ($\Delta M_{SECT} = 32.87$) (Figure 4b). This can be explained by the fact that the amount of moisture loss was more sensitive to the increasing of airflow rate when $V_{inlet} < 1.5 m \cdot s^{-1}$, which was caused by the significant decrease in peach surface average cooling rate (*i.e.*, more heat transfer fluxes) for this range of airflow rate (Figure 4c). Additionally, it was also further verified that the range of 1.5 - 2.5 $m \cdot s^{-1}$ was more beneficial for peach precooling to maintain the fresh quality, and improve the edible taste. Besides, the improvement rate of overall cooling uniformity between 1.5 and 2.5 $m \cdot s^{-1}$ was also three-fold of that in 0.5 - 1.5 $m \cdot s^{-1}$, thus indicating the inversely proportional relationship between cooling uniformity and moisture loss.

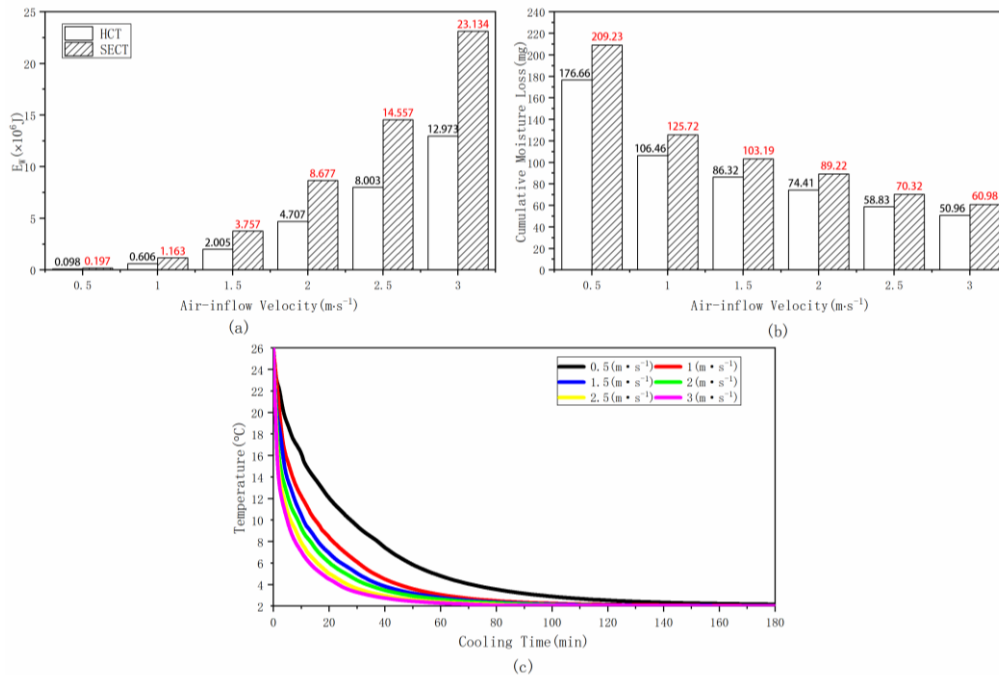


Figure 4. (a) Cumulative histogram of energy consumption (E_w , $\times 10^6$ J) for individual carton; (b) moisture loss (M , mg) of peach (1-1) as a function of different air-inflow velocities during the HCT and SECT; and (c) surface area-weighted average temperature of peach (1-1).

There was only a small difference of water evaporation between HCT and SECT, even if SECT took about twice as long as HCT (Figures 2a and 4b). This could be due to the fact that the changing trend of temperature difference (HI'_t) was increased to the maximum first (*i.e.*, the position of maximum hot spots and minimum cold spots were approximately at $Y_{avg} = 0.4$, which was closed to HCT), and subsequently decreased slowly for a short time (Figure 3), namely, the convective heat transfer between peach and refrigerated air mainly occurred in HCT. Moreover, mass loss was inversely proportional to air-inflow velocity for the reason that HCT and SECT were both decreased with a substantial increase in airflow rate. The amount of moisture loss was considerably small, and the maximum loss was only as high as 0.11%, which is far lower than 1% of most FAC procedures (Thompson *et al.*, 2008). This could be due to the high humidity over short precooling duration, that was, $RH = 90\%$ in this numerical model, and for peach precooling, SECT was mainly concentrated at 2.5 h when $V_{inlet} > 0.5 m \cdot s^{-1}$.

Conclusion

To conclude, a multi-parameter evaluation system was proposed to improve and understand the

comprehensive influence of different air-inflow velocities on peach cooling efficiency. Based on the obtained results, the decrease in accumulative water evaporation was largely associated with the increase in airflow rate, despite that its downtrend was becoming relatively constant when $V_{inlet} > 1.5 m \cdot s^{-1}$. Meanwhile, the uniformity was significantly promoted by three-fold of that in 0.5 - 1.5 $m \cdot s^{-1}$ when airflow rate was increased from 1.5 to 2.5 $m \cdot s^{-1}$. Coupled with little impact on SECT and heat transfer flux across the peach surface, any further increase in air-inflow velocity wasted the extra energy requirements. Hence, the airflow rate of 1.5 - 2.5 $m \cdot s^{-1}$ was more suitable to enhance the fresh quality and safety, and also to minimise unnecessary energy requirements during the FAC of peach.

Furthermore, for peach precooling, the mass loss mainly occurred in HCT, and was inversely proportional to cooling uniformity and airflow rate. Energy consumption is a power-law function, and appeared as an infinite growth trend with an increase in air-inflow velocity. Finally, the proposed novel evaluation system provided a reliable theoretical basis for researchers to optimise the precooling strategy, and to enhance the edible value of other spherical horticultural fruits postharvest.

Acknowledgments

This work was funded by the National Key Technology Research and Development Program of China (No. 2018YFD0700300) and Doctoral Research Initiation Project of Shanxi Agricultural University (No. 2021BQ86).

References

- Becker, B. R., Misra, A. and Fricke, B. A. 1996. Bulk refrigeration of fruits and vegetables part I: theoretical considerations of heat and mass transfer. *HVAC&R Research* 2(2): 122-134.
- Berry, T. M., Defraeye, T., Nicolai, B. M. and Opara, U. L. 2016. Multi-parameter analysis of cooling efficiency of ventilated fruit cartons using CFD: impact of vent hole design and internal packaging. *Food and Bioprocess Technology* 9(9): 1481-1493.
- Berry, T. M., Delele, M. A., Griessel, H. and Opara, U. L. 2015. Geometric design characterisation of ventilated multi-scale packaging used in the South African pome fruit industry. *Agricultural Mechanization in Asia, Africa, and Latin America* 46(3): 34-42.
- Brosnan, T. and Sun, D. W. 2001. Precooling techniques and applications for horticultural products - a review. *International Journal of Refrigeration* 24(2): 154-170.
- De Castro, L. R., Vigneault, C. and Cortez, L. A. B. 2004. Container opening design for horticultural produce cooling efficiency. *Journal of Food, Agriculture and Environment* 2(1): 135-140.
- Defraeye, T., Cronjé, P., Berry, T., Opara, U. L., East, A., Hertog, M., ... and Nicolai, B. 2015a. Towards integrated performance evaluation of future packaging for fresh produce in the cold chain. *Trends in Food Science and Technology* 44(2): 201-225.
- Defraeye, T., Lambrecht, R., Tsige, A. A., Delele, M. A., Opara, U. L., Cronjé, P., ... and Nicolai, B. 2013. Forced-convective cooling of citrus fruit: package design. *Journal of Food Engineering* 118(1): 8-18.
- Defraeye, T., Verboven, P., Opara, U. L., Nicolai, B. M. and Cronjé, P. 2015b. Feasibility of ambient loading of citrus fruit into refrigerated containers for cooling during marine transport. *Biosystems Engineering* 134: 20-30.
- Dehghannya, J., Ngadi, M. and Vigneault, C. 2008. Simultaneous aerodynamic and thermal analysis during cooling of stacked spheres inside ventilated packages. *Chemical Engineering Technology* 31(11): 1651-1659.
- Dehghannya, J., Ngadi, M. and Vigneault, C. 2010. Mathematical modeling procedures for airflow, heat and mass transfer during forced convection cooling of produce - a review. *Food Engineering Reviews* 2(4): 227-243.
- Dehghannya, J., Ngadi, M. and Vigneault, C. 2011. Mathematical modeling of airflow and heat transfer during forced convection cooling of produce considering various package vent areas. *Food Control* 22(8): 1393-1399.
- Delele, M. A., Ngcobo, M. E. K., Getahun, S. T., Chen, L., Mellmann, J. and Opara, U. L. 2013a. Studying airflow and heat transfer characteristics of a horticultural produce packaging system using a 3-D CFD model. Part I - model development and validation. *Postharvest Biology and Technology* 86: 536-545.
- Delele, M. A., Ngcobo, M. E. K., Getahun, S. T., Chen, L., Mellmann, J. and Opara, U. L. 2013b. Studying airflow and heat transfer characteristics of a horticultural produce packaging system using a 3-D CFD model. Part II - effect of package design. *Postharvest Biology and Technology* 86: 546-555.
- Dincer, I. 1995. Air flow precooling of individual grapes. *Journal of Food Engineering* 26(2): 243-249.
- Ferrua, M. J. and Singh, R. P. 2009. Modeling the forced-air cooling process of fresh strawberry packages, part I - numerical model. *International Journal of Refrigeration* 32: 335-348.
- Han, J. W., Badía-Melis, R., Yang, X. T., Ruiz-Garcia, L., Qian, J. P. and Zhao, C. J. 2017b. CFD simulation of airflow and heat transfer during forced-air precooling of apples. *Journal of Food Process Engineering* 40(2): article ID e12390.
- Han, J. W., Qian, J. P., Zhao, C. J., Yang, X. T. and Fan, B. L. 2017a. Mathematical modelling of cooling efficiency of ventilated packaging: integral performance evaluation. *International Journal of Heat and Mass Transfer* 111: 386-397.

- Han, J. W., Zhao, C. J., Qian, J. P., Ruiz-Garcia, L. and Zhang, X. 2018. Numerical modeling of forced-air cooling of palletized apple: integral evaluation of cooling efficiency. *International Journal of Refrigeration* 89: 131-141.
- Hoang, M. L., Verboven, P., Baelmans, M. and Nicolai, B. M. 2003. A continuum model for airflow, heat and mass transfer in bulk of chicory roots. *Transaction of the ASAE* 46(6): 1603-1611.
- Kongwong, P., Boonyakiat, D. and Poonlarp, P. 2019. Extending the shelf life and qualities of baby cos lettuce using commercial precooling systems. *Postharvest Biology and Technology* 150: 60-70.
- Lurie, S. and Crisosto, C. H. 2005. Chilling injury in peach and nectarine. *Postharvest Biology and Technology* 37(3): 195-208.
- Nahor, H. B., Hoang, M. L., Verboven, P., Baelmans, M. and Nicolai, B. M. 2005. CFD model of the airflow, heat and mass transfer in cool stores. *International Journal of Refrigeration* 28(3): 368-380.
- Norton, T., Sun, D. W., Grant, J., Fallon, R. and Dodd, V. 2007. Applications of computational fluid dynamics (CFD) in the modelling and design of ventilation systems in the agricultural industry: a review. *Bioresource Technology* 98(12): 2386-2414.
- O'Sullivan, J. L., Ferrua, M. J., Love, R. J., Verboven, P., Nicolai, B. M. and East, A. R. 2016. Modelling the forced-air cooling mechanisms and performance of polylined horticultural produce. *Postharvest Biology and Technology* 120: 23-35.
- O'Sullivan, J. L., Ferrua, M. J., Love, R. J., Verboven, P., Nicolai, B. M. and East, A. R. 2017. Forced-air cooling of polylined horticultural produce: optimal cooling conditions and package design. *Postharvest Biology and Technology* 126: 67-75.
- Olatunji, J. R., Love, R. J., Shim, Y. M., Ferrua, M. J. and East, A. R. 2017. Quantifying and visualising variation in batch operations: a new heterogeneity index. *Journal of Food Engineering* 196: 81-93.
- Ravindra, M. R. and Goswami, T. K. 2008. Comparative performance of precooling methods for the storage of mangoes. *Journal of Food Process Engineering* 31(3): 354-371.
- Rennie, T. J. and Tavoularis, S. 2009. Perforation-mediated modified atmosphere packaging: part I - development of a mathematical model. *Postharvest Biology and Technology* 51(1): 1-9.
- Shinya, P., Contador, L., Frett, T. and Infante, R. 2014. Effect of prolonged cold storage on the sensory quality of peach and nectarine. *Postharvest Biology and Technology* 95: 7-12.
- Thompson, J. F., Mejia, D. C. and Singh, R. P. 2010. Energy use of commercial forced-air coolers for fruit. *Applied Engineering in Agriculture* 26(5): 919-924.
- Thompson, J. F., Mitchell, F. G. and Rumsey, T. R. 2008. Commercial cooling of fruits, vegetables, and flowers. United States: UCANR Publications.
- Tutar, M., Erdogdu, F. and Toka, B. 2009. Computational modeling of airflow patterns and heat transfer prediction through stacked layers products in a vented box during cooling. *International Journal of Refrigeration* 32(2): 295-306.
- Wu, W. T., Haller, P., Cronj, P. and Defraeye, T. 2018. Full-scale experiments in forced-air precoolers for citrus fruit: impact of packaging design and fruit size on cooling rate and heterogeneity. *Biosystems Engineering* 169: 115-125.
- Yu, L. N., Liu, H. X., Shao, X. F., Yu, F., Wei, Y. Z., Ni, Z. M., ... and Wang, H. F. 2016. Effects of hot air and methyl jasmonate treatment on the metabolism of soluble sugars in peach fruit during cold storage. *Postharvest Biology and Technology* 113: 8-16.
- Zhao, C. J., Han, J. W., Yang, X. T., Qian, J. P. and Fan, B. L. 2016. A review of computational fluid dynamics for forced-air cooling process. *Applied Energy* 168: 314-331.
- Zhou, D. D., Sun, Y., Li, M. Y., Zhu, T. and Tu, K. 2019. Postharvest hot air and UV-C treatments enhance aroma-related volatiles by simulating the lipoxygenase pathway in peaches during cold storage. *Food Chemistry* 292: 294-303.